Optics & Laser Technology 197 (2026) 114794

Contents lists available at ScienceDirect

Optics and Laser Technology

journal homepage: www.elsevier.com/locate/jolt

Full length article

Few-cycle THz pulse generation in DSTMS driven by an 8.3-MHz amplified Mamyshev oscillator

Francesco Canella [a], Dario Giannotti [b,c,*], Sara Pizzurro [d], Riccardo Gotti [d], Lorenzo Mosesso [e,f], Stefano Lupi [e,f], Antonio Agnesi [d], Federico Pirzio [d], Gianluca Galzerano [a,c]

[a] Istituto di Fotonica e Nanotecnologie, Consiglio Nazionale delle Ricerche, Piazza Leonardo da Vinci 32, Milano, 20133, Italy
[b] Dipartimento di Fisica, Politecnico di Milano, Piazza Leonardo da Vinci 32, Milano, 20133, Italy
[c] Istituto Nazionale di Fisica Nucleare, Sezione di Milano, Via Celoria 16, Milano, 20133, Italy
[d] Dipartimento di Ingegneria Industriale e dell'Informazione, Università di Pavia, Via Ferrata 5, Pavia, 27100, Italy
[e] Dipartimento di Fisica, Università degli Studi di Roma "La Sapienza", P.Le Aldo Moro 5, Roma, 00185, Italy
[f] Istituto Nazionale di Fisica Nucleare, Sezione di Roma, P.Le Aldo Moro 2, Roma, 00185, Italy

ARTICLE INFO

Keywords:
THz generation
Mamyshev oscillator
DSTMS
Nonlinear optics
Optical rectification

ABSTRACT

Mamyshev oscillators are an emerging class of ultrafast fiber lasers that support exceptionally broadband spectra and few-femtosecond pulse durations, making them well-suited for nonlinear frequency conversion. Despite this potential, THz generation with Mamyshev oscillators has not been demonstrated to date. In this work, we report the generation of THz few-cycle pulses at an 8.3 MHz repetition rate via optical rectification of a 31-fs pulse duration, 1-W average power amplified Mamyshev oscillator in a 190-μm-thick DSTMS organic crystal. We measure a THz average power of 40 μW and a spectral bandwidth of 4 THz. To further investigate the advantages of combining the Mamyshev oscillator and organic crystals for THz generation at a multi-MHz repetition rate, we compare the THz pulses with those generated using a conventional inorganic 500 μm-thick GaP crystal, obtaining comparable bandwidth, but 20 times lower power with respect to DSTMS.

1. Introduction

Ultrafast lasers are today the cornerstone of several scientific fields and applications, such as ultrafast spectroscopy, laser micromachining, and nonlinear optics [1]. In recent years, ultrafast ytterbium-doped fiber lasers have become increasingly popular due to their stability, compactness, and robustness compared to solid-state lasers. Mamyshev oscillators (MOs) in fiber represent a cutting-edge advancement in contemporary ultrafast fiber laser technology at 1 μm wavelength, offering excellent performance in pulse energy (>100 nJ), very large nonlinear phase (on the order of 100π), and high-quality compressibility down to ~30 fs duration [2,3]. Furthermore, MOs are generally less sensitive to environmental noise compared to other common architectures based on nonlinear polarization evolution, the use of SESAMs, or nonlinear optical loop mirrors [4], due to their operating principle relying on spectral filtering rather than polarization-dependent effects [5] One of the main challenges in MOs is initiating the mode-locking regime, which is often achieved through complex techniques such as the injection of a short picosecond pulse produced by another mode-locked oscillator or pump modulation. Only recently, a sub-ns passively Q-switched external starter has been successfully employed as a simple, robust, and cost-effective solution to reliably initiate the mode-locking regime, even in high-gain configurations based on large-mode-area fibers [6,7]. The recent discovery of the pulse propagation regime known as gain-managed nonlinear amplification (GMNA) has enabled further significant advances [8]. Indeed, a proper pulse amplification is essential to transfer the attractive features of MOs to applications where high energy is required, overcoming the intrinsic limits of traditional approaches like chirped-pulse-amplification. The peculiarity of the GMNA regime is the interplay of positive dispersion and spectral gain evolution with pulse amplification along the fiber to reach a spectral bandwidth beyond the gain bandwidth of the amplifier itself. We have recently shown that by selecting with a band-pass filter the proper seeding wavelength within the spectrum of the MO, it is possible to optimize the performance of the GMNA amplifier in terms of suppression of the compressed pulse pedestal and minimization of the

* Corresponding author at: Dipartimento di Fisica, Politecnico di Milano, Piazza Leonardo da Vinci 32, Milano, 20133, Italy.
Email address: dario.giannotti@polimi.it (D. Giannotti).

https://doi.org/10.1016/j.optlastec.2026.114794
Received 12 December 2025; Received in revised form 12 January 2026; Accepted 19 January 2026
Available online 27 January 2026

pulse duration, resulting in a higher pulse peak power [9] with respect to Refs. [6,7]. These features make GMNA amplifiers seeded by MOs particularly well-suited for nonlinear optics experiments, such as mid-infrared optical parametric generation and laser-driven terahertz wave (THz) generation via optical rectification (OR) in $\chi^{(2)}$ crystals [10,11]. Photoconductive antennas (PCAs) constitute an alternative tabletop approach to THz generation and detection. Recent developments, such as large-area and micro-structured PCAs, have enabled very high dynamic ranges and milliwatt-level average powers at repetition rates ranging from hundreds of kHz up to the MHz regime [12,13]. However, a fair comparison between PCA and OR sources is not straightforward, as they rely on fundamentally different emission mechanisms that result in different temporal dynamics and operational regimes. Moreover, the emission peak frequency rarely exceeds 1 THz. Nevertheless, to the best of our knowledge, no OR experiments with Mamyshev oscillators have been reported to date. This application of MOs is of great interest, since ultrafast laser-driven few-cycle THz pulse sources are now widely recognized as essential instruments in many areas of fundamental and applied research, as well as technological and industrial applications [14]. The $\chi^{(2)}$ nonlinear crystals are widely available on the market. A wise choice of both the crystal and the pump laser (wavelength, pulse duration, pulse energy, and repetition rate) is critical for defining the achievable THz bandwidth, pulse energy, and data-acquisition speed. All these parameters need to be balanced to maximize the dynamic range and the signal-to-noise ratio (SNR) of THz spectroscopic measurements [15]. High bandwidth ($>$ 4 THz) is usually obtained at the expense of the dynamic range with thin crystals, while high energy is achieved at the expense of the repetition rate of the pump laser, which can degrade the SNR unless acquisition times are extended significantly [16]. Notably, SNR in time-domain spectroscopy scales both with the single pulse amplitude (favoring higher pulse energy) and with the square root of the number of averaged shots (favoring higher repetition rates). Consequently, operation at hundreds of kHz can be advantageous for experiments limited by pulse amplitude, detector linearity saturation, or single-shot measurements. On the other hand, MHz operation allows the acquisition of sampling orders of magnitude higher. THz pulses at high repetition rates can also be exploited in a dual comb configuration [17]. Such measurements allow for fast data collection with no limitations given by mechanical delay lines or a shaker, typically involved in time-domain THz spectroscopy setups. Moreover, increasing the pulse energy is not always desirable: higher peak intensities may drive unwanted nonlinearities in the generation crystal, increase the risk of optical damage, or require more complex dispersion handling and damage-mitigation strategies.

Average power levels on the order of mW at repetition rates exceeding tens of MHz have been demonstrated with OR of thin $LiNbO_3$ (lithium niobate) plates or gallium phosphide (GaP) inside active and passive optical cavities [18–20]. Cavities boost the pulse energy at high repetition rates, but they require specific know-how and electro-optical components to work properly. For this reason, for future technology scalability, single-pass OR still remains the simplest and preferable option. In this context, organic crystals have emerged as excellent alternative candidates to traditionally used inorganic crystals (mainly GaP, $LiNbO_3$, ZnTe, and GaSe), since they combine the advantages of a broad generation bandwidth in a simple collinear geometry with high conversion efficiency. The most common organic crystals used for OR pumped by near-infrared lasers are DSTMS (4-N,N-dimethylamino4'-N'-methyl-stilbazolium 2,4,6 trimethylbenzenesulfonate), BNA (N-benzyl-2-methyl-4-nitroaniline), OH1 (2-[3-(4 hydroxystyryl)-5,5dimet- hylcyclohex-2-enylidene] malononitrile), HMQ-TMS (2-(4-hydroxy-3-methoxys- tyryl)-1-methilquinolinium 2,4,6-trimethylbenzenesulfonate), and DAST (4-N,N-dimethylamino-4'-N'-methyl-stilbazolium tosylate). Comprehensive information on organic crystals can be found in Ref. [21]. Note that the high conversion efficiency is mainly due to a large effective nonlinear coefficient d_{eff}, which contributes quadratically to the conversion efficiency [11]. E.g., GaP has a d_{eff} = 24 pm V^{-1}, while DSTMS has d_{eff} = 230 pm V^{-1} [16]. Among inorganic crystals, $LiNbO_3$ is a special case, since it has a high d_{eff} = 160 pm V^{-1}, but it is out of phase matching in almost all the near infrared region. As a drawback, organic crystals are sensitive to high average power: specific substrates or chopping are often required to avoid thermal damage [22]. The literature reports several notable examples of high-repetition-rate THz generation using organic crystals pumped by a Yb lasers. Among them, in Ref. [23], Buchmann et al. demonstrated the generation of mW-level quasi-single-cycle THz pulses at a 10-MHz repetition rate via OR in HMQ-TMS, pumped by a Yb-fiber laser whose pulses were recompressed by a multipass cell to 22 fs. In 2021, Mansourzadeh et al. [22] proved 0.95 mW of THz at a 13-MHz repetition rate using a high-power thin-disk laser and a BNA. With a 100-kHz repetition rate, Wang et al. [24] have recently demonstrated strong field THz using a DSTMS crystal (other relevant studies on DSTMS exploited lasers at repetition rates significantly below the MHz and at longer wavelength [25–27]). However, a study of OR in DSTMS with Yb lasers at MHz repetition rates is still unpublished.

In this work, we report THz generation via OR in DSTMS and GaP crystals exploiting a compact (20×30 cm^2 footprint, air cooled) Yb-doped fiber laser system based on a MO amplified in the GMNA regime. Our pump laser source delivers high-quality pulses compressible to 31 fs without side lobes, reaching peak power up to 4 MW at 1 μm. Although the phase-matching at 1 μm is not optimal in DSTMS, our measurements show that the OR process still yields stable and reproducible THz emission at multi-MHz repetition rates, with average power in the tens of μW range and an emission peak beyond 2 THz, demonstrating that this configuration remains practically effective despite its intrinsic limitations. Further studies will be conducted on other organic crystals with different properties in terms of efficiency and phase-matching.

2. Experimental setup

The setup of THz generation is shown in Fig. 1. The band-pass filter selects approximately 3 nm FWHM portion of the ~25-nm wide MO spectrum to seed the GMNA amplifier with the resulting 2-mW average power pulse train. The wide spectrum of the MO allows a fine tuning of the seeding wavelength which helps optimize the performance of the GMNA fiber amplifier [9]. The spectrally-filtered output of the MO is amplified to 1.1 W in a Yb-doped fiber amplifier pumped by a 7-W multimode diode at 976 nm. After amplification, the pulses are compressed to a minimum duration of 31 fs by a grating pair (1000 grooves/mm, single pass transmission >97% at 1040 nm) in the Treacy configuration [28]. The second-harmonic intensity autocorrelation and the spectrum of the amplified pulses are shown in Fig. 2, in panels (a) and (b), respectively. The autocorrelation is well fitted by a Sech^2 profile, which highlights the excellent quality of the pulse. The optical spectrum has a FWHM > 80 nm, and in log-scale it extends from ~ 1 μm to above 1.2 μm (signal-to-noise ratio ≈ 40 dB). An extensive description of the GMNA seeded by a MO can be found in Refs. [9,29]. To generate THz, the amplified pulses are selected in polarization with a half-wave plate (HWP) and a polarizing beam splitter (PBS). Then, the beam passes through a mechanical chopper with selectable frequency and duty cycle and is focused by a 200-mm focal length lens into a DSTMS organic crystal for single-pass collinear OR. For comparison, the DSTMS can be substituted by a GaP placed in the same configuration. The 190-μm-thick, uncoated DSTMS (SwissTHz) is placed on a rotating mount to optimize the angle of phase matching. The organic crystal is deposited on a millimetric silica substrate, and its thickness is chosen to stay within the coherence length up to 5 THz pumping at 1–1.1 μm. Inside the crystal, the dimension of the waist of the laser is w_{IR} = 100 μm. The THz radiation diverges from a dimension of $w_{\text{THz}} = w_{\text{IR}}/\sqrt{2} \approx 70$ μm and is collected by a protected gold off-axis-parabolic mirror (OAP) of focal length and diameter of 50.8 mm. The infrared beam is discarded by a 3-mm hole in the center of the OAP (without significant THz losses). We estimate that

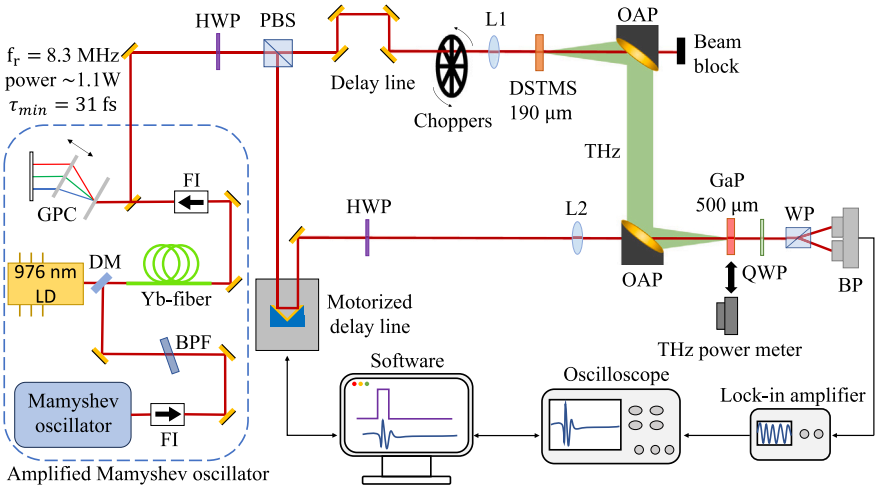

Fig. 1. Experimental setup schematics. BPF: band-pass filter; FI: Faraday isolator; DM: dichroic mirror; GPC: grating pair compressor; H/QWP: half/quarter-wave plate; PBS: polarizing beam splitter; L1 and L2: lenses f = 200 mm; OAP: off-axis parabolic mirror; WP: Wollaston prism; BP: balanced photodiode.

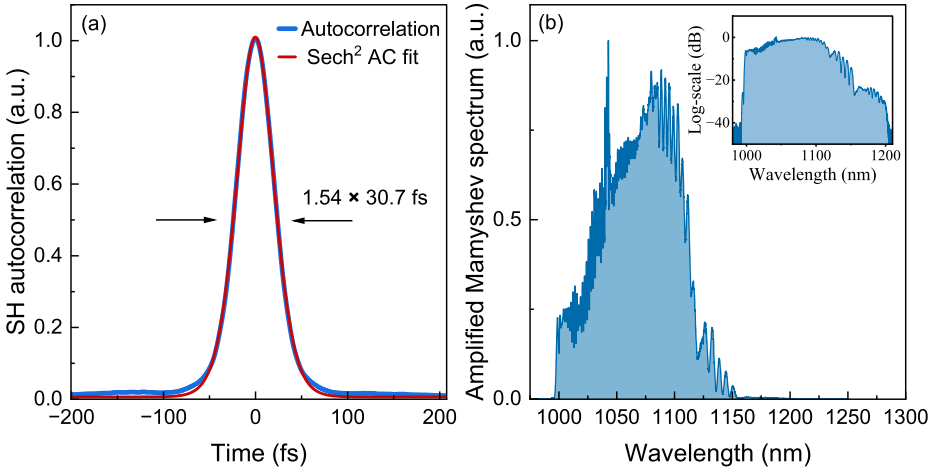

Fig. 2. Amplified Mamyshev oscillator: (a) SH intensity autocorrelation with Sech^2 fit, and (b) spectrum in linear and log scale (inset).

the divergence of the THz beam (especially below 1 THz) causes a loss of ~50–55% of power [30]. The first OAP collimates the THz, while a second identical OAP focuses the beam for applications and characterization. The distance between the two OAPs is twice their focal length (101.6 mm). At the focal point, we performed the characterization of the generated pulses in terms of average power (using a THz power meter) and in terms of pulse shape and spectrum through electro-optical sampling (EOS) [31]. For power characterization, we used a pyroelectric power meter (Ophir RM9-THz), with a noise floor of about 200 nW. The detector operates with a dedicated beam chopper at 18 Hz and 50% duty cycle. To block residual scattered infrared radiation, while maintaining partial THz transmission, we have inserted two calibrated infrared-blocking sheets that transmit 26% of the THz signal. The THz beam waist at the second OAP focus, measured using the knife-edge method, is ~420 µm.

3. THz generation results

Fig. 3(a) shows the generated THz average power as a function of the pumping infrared power. The power out of the fiber amplifier sent to the DSTMS crystal is controlled with the HWP and PBS placed at the output of the amplified MO. The pump power is changed from a few mW to 1.02 W (slightly lower than at the amplifier's output due to residual losses of the broadband metallic mirrors employed in the optical path). For all measurements, the chopper rotates at 18 Hz with a 50% duty cycle, halving the effective average power without affecting the pulse energy, which reached 120 nJ at maximum. The maximum THz power generated is 40 µW, corresponding to a peak electric field of 1.63 kV m^{-1} at the focus. As expected from an OR process, the trend is purely quadratic as a function of the pump power. The infrared pulse is pre-chirped by −600 fs^2 to empirically maximize THz generation, achieving the minimum pulse duration inside the generation crystal. If no pre-chirp is applied, the power significantly drops (more than −50%) as the estimated pulse duration inside the crystal is about 150 fs due to its dispersion. Efficiency saturation owing to thermal load is an important element that must be taken into account when using organic crystals. For instance, Ref. [22] shows a strong conversion efficiency saturation of a BNA crystal for a duty cycle >20% and an effective repetition rate of 2.7 MHz, while Ref. [27] reports simulations and experiments on the absorption mechanisms of DSTMS at increasing pump fluence. To investigate whether heat accumulation limits THz generation, we measured the average THz power as a function of the chopper duty cycle. The results are shown in Fig. 3(b). To perform the measurement, a second chopper with variable blade coverage and high rotation speed (up to 1 kHz) is inserted into the beam path (in line after the 18-Hz chopper) to modulate the duty cycle between 10% and 50%, effectively varying

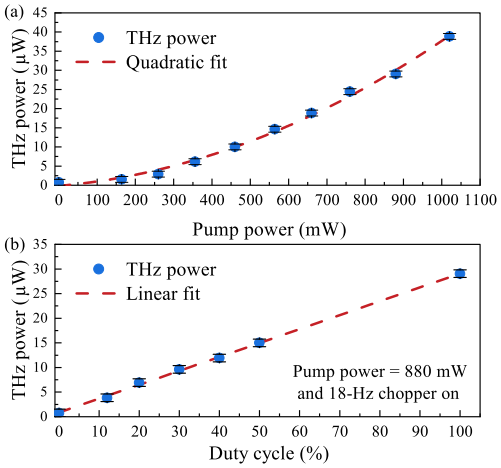

Fig. 3. (a) THz average power measured with the pyroelectric power meter as a function of the infrared pump power (solid points). The data are fitted with a quadratic curve (dashed line). (b) THz average power as a function of the second chopper's duty cycle (solid points). The black error bars indicate the power meter uncertainty of 0.2 μW. The data are fitted with a linear curve (dashed line). The infrared pump power is kept constant to 880 mW with the 18-Hz chopper on.

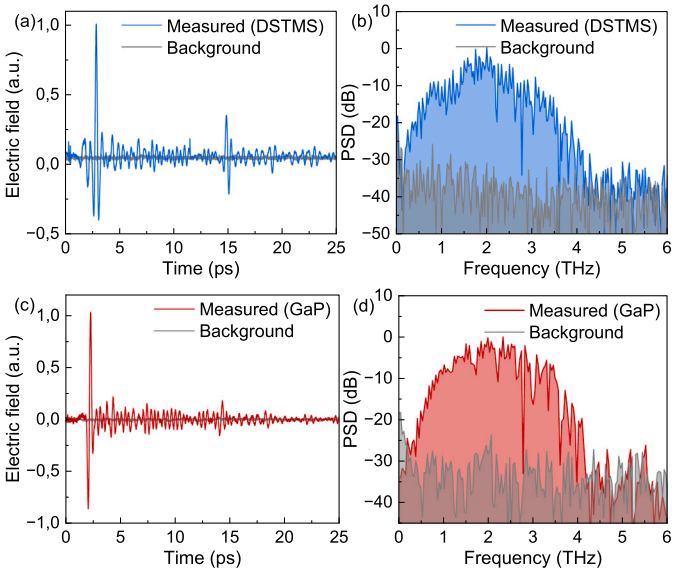

Fig. 4. Electro-optical sampling of THz pulses and spectrum. Panels (a) and (c): Temporal traces of THz pulse generated with DSTMS and GaP, respectively. Panels (b) and (d): Power spectral density of the THz pulses generated with DSTMS and GaP, respectively.

the duration of the burst of infrared pulses. This way, the crystal experiences different ratios of generation time and cooling time for heat dissipation. In numbers, for a cycle of 1 ms, at a 10% duty cycle, the resting time is 900 μs, while at a 50% duty cycle it is 500 μs. The pump is kept constant at 880 mW with the slow 18-Hz chopper on, and the energy per pulse remains unchanged across all measurements. The 18-Hz chopper does not affect the measurement, since its rotation has a time scale 100 times slower than the thermal dynamics in DSTMS. At a 50% duty cycle, the THz generated is ~15 μW. The point of highest power is acquired by removing the second chopper (equivalent to a duty cycle of 100%), obtaining ~ 30 μW of THz. The geometry of the variable blade does not allow for variations of the duty cycle between 50% and 100%. We observed no significant saturation effects, in line with the studies of Refs. [27,32]. Indeed, given the maximum average power and fluence (< 2 mJ/cm^2) in our setup, effects such as cascaded OR and multiphoton absorption remain marginal compared to the THz generation process. Even though we observed no performance degradation of the DSTMS crystal during our experimental campaign, more systematic studies on THz power stability and crystal reliability over long periods will be conducted in the future.

For comparison, we generated THz using a conventional inorganic 500-μm-thick GaP crystal, AR-coated for the pump wavelength (EKSMA Optics). The GaP sample thickness was chosen to compare the two materials at a similar bandwidth [33]. In addition, thinner GaP crystals would generate THz pulses that are barely detectable by the pyroelectric detector. In this case, the maximum average power measured after the OAPs with the pyroelectric power meter is 2.3 μW, more than 17 times lower compared to the case of DSTMS. As a second set of characterization measurements, we acquired the EOS trace of the THz pulses. The EOS is performed by extracting less than 10% of the power from the PBS at the output of the GMNA amplifier. This laser beam goes to a motorized delay line, then it is focused (with a lens of 200-mm focal length) and recombined with the THz pulses in an AR-coated 500-μm GaP crystal. The detection crystal length used is the shortest available in the lab, selected to optimize phase-matching and thereby the detection bandwidth [33]. Nevertheless, we estimate that the THz generated with DSTMS is slightly attenuated above 4 THz due to this limitation. When the laser and THz fields are properly overlapped and oriented in the crystal, the Pockels effect causes a change in the EOS crystal's refractive index, inducing a slight ellipticity of the laser beam polarization, making the THz electric field detectable. Both fields are linearly polarized at the interaction point. A quarter-wave plate and a Wollaston prism separate the two polarization components, which are sent to a balanced photodiode. The output of the photodiode is proportional to the THz field synchronized with the infrared beam. By scanning the delay between the THz and the probe beam, the full temporal waveform can be acquired with an oscilloscope. To ensure synchronization between the THz and the probe beam, the beam used for OR travels a delay line (see Fig. 1). Data are acquired using a lock-in amplifier (Stanford Research Systems SR530) with 1 s integration time, connected to an oscilloscope. In this case, the chopper modulates the THz at 10 kHz while triggering the lock-in. The same computer synchronizes the motorized delay line and the data acquisition. The delay line slowly drifts at a speed of 10 μm/s in a range of a few millimeters, corresponding to tens of ps of optical delay. The EOS traces of the THz pulses generated by the DSTMS and the comparison GaP are shown in Fig. 4, respectively in panels (a) and (c). Both traces exhibit few-cycle oscillations of the THz field, followed by longer oscillations characteristic of atmospheric water-vapor absorption, as well as a secondary replica of the main pulse at a delay of approximately 15 ps. The latter is the etalon effect of the THz pulse inside the sampling GaP and is mainly due to the AR-coating for the infrared pump, and more pronounced for the DSTMS measurement. We attribute the different amplitude of the replica produced by the etalon effect to inhomogeneities in the GaP coating, which can cause reflections of varying intensity. From the temporal traces, it is possible to extract the power spectral density (PSD) via the Fourier transform. The spectrum of the THz pulses generated with DSTMS and GaP are shown in logarithmic scale in panels (b) and (d), respectively. Both spectra span from quasi-DC frequencies (below 500 GHz) to above 4 THz. The spectrum of THz from GaP has a more regular shape, while THz from DSTMS shows dips around 1.5 and 2.5 THz, corresponding to the absorption peaks of such a crystal [24,34]. In both cases, there is a modulation at 75 GHz, due to the aforementioned parasitic etalon effect in the sampling crystal.

The spectrum of THz from DSTMS extends below 250 GHz at low frequencies, and some power is visible at around 5 THz, after the phase-matching bounce to zero signal at 4.3 THz. For both spectra, the signal-to-noise ratio exceeds 30 dB. The water absorption peaks are clearly visible in both spectra, with strong lines at 1.7, 2.2, 2.6, 2.8, 3.1, and

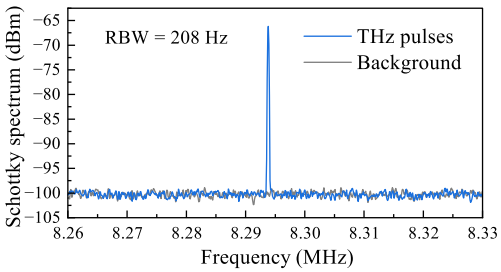

Fig. 5. Power spectrum of THz radiation from DSTMS acquired with Schottky diode. The resolution bandwidth (RBW) is 208 Hz.

3.6 THz. The comparison between the two spectra shows no significant differences between the performances of DSTMS and GaP, despite a ~20-fold difference in THz power, in good agreement with the efficiency ratio of a factor of ~30 [16]. This demonstrates the strong potential of amplified MO for seeding OR in organic crystals at MHz-repetition rate, opening promising perspectives for compact time-domain spectrometers based on this technology.

As a final measurement, we acquired the power spectrum of THz pulses from DSTMS around the repetition rate, using a quasi-optical Schottky diode (3DL-12C-LS2500-A1, ACST) and an electrical spectrum analyzer (Agilent E4445A). The Schottky diode has an electrical bandwidth of 1 MHz, and an optical bandwidth of a few THz. The diode directly measures THz pulses and it is blind in the infrared (no chopper or lock-in are required). Fig. 5 shows the repetition rate peak at 8.3 MHz measured with a resolution bandwidth of 208 Hz. The signal-to-noise ratio is high (~33 dB) despite measuring at frequencies beyond the detector's electrical bandwidth (attenuation ~20 dB). Apart from the sharp peak of the repetition rate at 8.3 MHz, no additional noise is observed above the detection limit, showing no significant noise degradation in the OR process. This result agrees with the GMNA amplified MO low-noise performance reported in Pizzurro et al. [9].

After the promising results of this work, future investigations will concentrate on long-term THz power stability, organic crystal performance over time, and temperature control strategies. Furthermore, tests with newly procured organic crystals (BNA, MNA) will be performed to systematically study the full potential of MO-based THz generation systems.

4. Conclusion

In summary, we demonstrate THz pulse generation at 8.3 MHz via OR in a 190-μm DSTMS crystal, driven by a 31-fs, 1.1-W amplified Mamyshev oscillator. We achieve a maximum THz average power of 40 μW with a spectral bandwidth exceeding 4 THz, few-cycle temporal profiles, and no significant noise degradation. Compared to a 500-μm GaP crystal, DSTMS yields almost 20-times higher output power with similar bandwidth, confirming the advantage of organic crystals for efficient, high-repetition-rate, broadband THz generation. This work opens promising prospects for Mamyshev-based compact, THz time-domain spectrometers operating at multi-MHz rates.

CRediT authorship contribution statement

Francesco Canella: Writing – review & editing, Writing – original draft, Investigation, Formal analysis, Data curation. **Dario Giannotti:** Writing – review & editing, Writing – original draft, Investigation, Formal analysis, Data curation. **Sara Pizzurro:** Writing – review & editing, Investigation, Data curation. **Riccardo Gotti:** Writing – review & editing, Investigation, Data curation. **Lorenzo Mosesso:** Investigation, Data curation. **Stefano Lupi:** Supervision. **Antonio Agnesi:** Writing – review & editing, Validation, Supervision, Funding acquisition, Conceptualization. **Federico Pirzio:** Writing – review & editing, Supervision, Investigation, Funding acquisition, Formal analysis. **Gianluca Galzerano:** Writing – review & editing, Validation, Supervision, Funding acquisition, Conceptualization.

Declaration of competing interest

The authors declare that they have no known competing financial interests or personal relationships that could have appeared to influence the work reported in this paper.

Acknowledgment

This work was supported by: the European Union's NextGenerationEU Program with the I-PHOQS Infrastructure [IR0000016, ID D2B8D520, CUP B53C2- 2001750006]; ATTILA - Advanced room-Temperature THz hyperspectral Imaging based on novel ultrafast fiber Lasers (20227849RL); and INFN CSN5, projects ETHIOPIA and ATHENAE.

Data availability

Data underlying the results presented in this paper are not publicly available at this time but may be obtained from the authors upon reasonable request.

References

[1] D.T. Reid, C.M. Heyl, R.R. Thomson, R. Trebino, G. Steinmeyer, H.H. Fielding, R. Holzwarth, Z. Zhang, P. Del'Haye, T. Südmeyer, G. Mourou, T. Tajima, D. Faccio, F.J.M. Harren, G. Cerullo, Roadmap on ultrafast Optics, J. Opt. 18 (9) (2016) 093006.
[2] P. Sidorenko, W. Fu, L.G. Wright, M. Olivier, F.W. Wise, Self-seeded, multi-megawatt, Mamyshev oscillator, Opt. Lett. 43 (11) (2018) 2672–2675.
[3] W. Liu, R. Liao, J. Zhao, J. Cui, Y. Song, C. Wang, M. Hu, Femtosecond Mamyshev oscillator with 10-mW-level peak power, Optica 6 (2) (2019) 194–197.
[4] A. Chong, L.G. Wright, F.W. Wise, Ultrafast fiber lasers based on self-similar pulse evolution: a review of current progress, Rep. Prog. Phys. 78 (11) (2015) 113901.
[5] Y.-Y. Li, B. Gao, C.-Y. Ma, G. Wu, J.-Y. Huo, Y. Han, S. Wageh, O.A. Al-Hartomy, A.G. Al-Sehemi, L. Liu, H. Zhang, Generation of high-peak-power femtosecond pulses in Mamyshev oscillators: recent advances and future challenges, Laser Phys. Rev. 17 (4) (2023) 2200596, https://doi.org/10.1002/lpor.202200596
[6] R. Gotti, L. Carrà, S. Pizzurro, G. Piccinno, A. Agnesi, F. Pirzio, 1MW peak-power Mamyshev oscillator started by a passively q-switched microchip laser, Adv. Photon. Res. 5 (11) (2024) 2400028.
[7] R. Gotti, S. Pizzurro, F. Canella, D. Giannotti, G. Galzerano, A. Agnesi, F. Pirzio, Femtosecond Mamyshev fiber oscillator started by ultra-low power microchip laser seeder at two different wavelengths: a comparison, Opt. Express. 32 (24) (2024) 43635–43642, https://doi.org/10.1364/OE.541946
[8] P. Sidorenko, W. Fu, F. Wise, Nonlinear ultrafast fiber amplifiers beyond the gain-narrowing limit, Optica 6 (10) (2019) 1328–1333.
[9] S. Pizzurro, R. Gotti, X. Ypi, F. Canella, D. Giannotti, G. Galzerano, A. Agnesi, F. Pirzio, Gain-managed nonlinear amplification and noise performance of an Yb-doped fiber amplifier seeded at different wavelengths, Opt. Laser Technol. 193 (2026) 114233, https://doi.org/10.1016/j.optlastec.2025.114233
[10] Sukeert, S. Pizzurro, A. Esteban-Martín, R. Gotti, L. Carrà, G. Piccinno, A. Agnesi, F. Pirzio, S.C. Kumar, M. Ebrahim-Zadeh, Efficient femtosecond optical parametric generation in group-velocity-matched mgo:ppln at 10 emhz, Opt. Lett. 48 (22) (2023) 6008–6011.
[11] J.A. Fülöp, S. Tzortzakis, T. Kampfrath, Laser-driven strong-field terahertz sources, Adv. Opt. Mater. 8 (3) (2020) 1900681.
[12] N.V. Zenchenko, D.V. Lavrukhin, R.R. Galiev, A.E. Yachmenev, R.A. Khabibullin, Y.G. Goncharov, I.N. Dolganova, V.N. Kurlov, T. Otsuji, K.I. Zaytsev, D.S. Ponomarev, Enhanced terahertz emission in a large-area photoconductive antenna through an array of tightly packed sapphire fibers, Appl. Phys. Lett. 124 (12) (2024) 121107.
[13] M. Khalili, Y. Wang, S. Winnerl, C.J. Saraceno, High-power single-cycle thz emission from large-area photoconductive emitters at 400 kHz, Opt. Lett. 50 (7) (2025) 2141–2144.
[14] P.U. Jepsen, D.G. Cooke, M. Koch, Terahertz spectroscopy and imaging – modern techniques and applications, Laser Photon. Rev. 5 (1) (2011) 124–166.
[15] P.U. Jepsen, B.M. Fischer, Dynamic range in terahertz time-domain transmission and reflection spectroscopy, Opt. Lett. 30 (1) (2005) 29–31.
[16] S. Mansourzadeh, T. Vogel, A. Omar, T.O. Buchmann, E.J.R. Kelleher, P.U. Jepsen, C.J. Saraceno, Towards intense ultra-broadband high repetition rate terahertz sources based on organic crystals - invited, Opt. Mater. Express 13 (11) (2023) 3287–3308.
[17] B. Willenberg, C.R. Phillips, J. Pupeikis, S.L. Camenzind, L. Liebermeister, R.B. Kohlhass, B. Globisch, U. Keller, THz-TDS with gigahertz Yb-based dual-comb lasers: noise analysis and mitigation strategies, Appl. Opt. 63 (15) (2024) 4144–4156.

[18] M. Hamrouni, J. Drs, N. Modsching, V.J. Wittwer, F. Labaye, T. Südmeyer, Intra-oscillator broadband THz generation in a compact ultrafast diode-pumped solid-state laser, Opt. Express. 29 (15) (2021) 23729–23735.
[19] Y. Wang, T. Vogel, M. Khalili, S. Mansourzadeh, K. Hasse, S. Suntsov, D. Kip, C.J. Saraceno, High-power intracavity single-cycle THz pulse generation using thin lithium niobate, Optica 10 (12) (2023) 1719–1722.
[20] E. Suerra, F. Canella, D. Giannotti, M. Khalili, Y. Wang, K. Hasse, S. Suntsov, D. Kip, C. Saraceno, S. Cialdi, G. Galzerano, Ytterbium-laser-driven THz generation in thin lithium niobate at 1.9 kW average power in a passive enhancement cavity, APL Photonics 10 (4) (2025) 046111, https://doi.org/10.1063/5.0252040
[21] M. Jazbinsek, U. Puc, A. Abina, A. Zidansek, Organic crystals for THz photonics, Appl. Sci. 9 (5) (2019), https://doi.org/10.3390/app9050882
[22] S. Mansourzadeh, T. Vogel, M. Shalaby, F. Wulf, C.J. Saraceno, Milliwatt average power, MHz-repetition rate, broadband THz generation in organic crystal BNA with diamond substrate, Opt. Express. 29 (24) (2021) 38946–38957.
[23] T.O. Buchmann, E.J. Railton Kelleher, M. Jazbinsek, B. Zhou, J.-H. Seok, O.-P. Kwon, F. Rotermund, P.U. Jepsen, High-power few-cycle THz generation at MHz repetition rates in an organic crystal, APL Photonics 5 (10) (2020) 106103.
[24] K. Wang, Z. Zheng, H. Li, X. Meng, Y. Liu, Y. Tian, L. Song, Efficient strong-field THz generation from DSTMS crystal pumped by 1030 NM yb-laser, Appl. Phys. Lett. 124 (12) (2024) 121102.
[25] C. Vicario, B. Monoszlai, C.P. Hauri, GV/m single-cycle terahertz fields from a laser-driven large-size partitioned organic crystal, Phys. Rev. Lett. 112 (2014) 213901.
[26] C. Vicario, A.V. Ovchinnikov, S.I. Ashitkov, M.B. Agranat, V.E. Fortov, C.P. Hauri, Generation of 0.9-mJ THz pulses in DSTMS pumped by a Cr:Mg2SiO4 laser, Opt. Lett. 39 (23) (2014) 6632–6635.
[27] J. Li, R. Rana, L. Zhu, C. Liu, H. Schneider, A. Pashkin, Limitation of THz conversion efficiency in DSTMS pumped by intense femtosecond pulses, Opt. Express. 29 (14) (2021) 22494–22503.
[28] E. Treacy, Optical pulse compression with diffraction gratings, IEEE J. Quantum Electron. 5 (9) (1969) 454–458.
[29] S. Pizzurro, R. Gotti, L. Carrà, G. Piccinno, A. Agnesi, F. Pirzio, Femtosecond Mamyshev fiber oscillator started by a passively q-switched microchip laser, Opt. Lett. 47 (8) (2022) 1960–1963, https://doi.org/10.1364/OL.457486
[30] J. Faure, J. Van Tilborg, R.A. Kaindl, W.P. Leemans, Modelling Laser-Based Table-Top THz sources: optical rectification, propagation and Electro-Optic sampling, Opt. Quantum Electron. 36 (8) (2004) 681–697.
[31] I.-C. Benea-Chelmus, J. Faist, A. Leitenstorfer, A.S. Moskalenko, I. Pupeza, D.V. Seletskiy, K.L. Vodopyanov, Electro-optic sampling of classical and quantum light, Optica 12 (4) (2025) 546–563.
[32] L. Mutter, F.D. Brunner, Z. Yang, M. Jazbinšek, P. Günter, Linear and nonlinear optical properties of the organic crystal DSTMS, J. Opt. Soc. Am. B 24 (9) (2007) 2556–2561.
[33] J. Drs, N. Modsching, C. Paradis, C. Kränkel, V.J. Wittwer, O. Razskazovskaya, T. Südmeyer, Optical rectification of ultrafast yb lasers: pushing power and bandwidth of terahertz generation in GaP, J. Opt. Soc. Am. B 36 (11) (2019) 3039, https://opg.optica.org/abstract.cfm?URI=josab-36-11-3039.
[34] G. Montemezzani, M. Alonzo, V. Coda, M. Jazbinsek, P. Günter, Running electric field gratings for detection of coherent radiation, J. Opt. Soc. Am. B 32 (6) (2015) 1078–1083.